
Imaging Taxane-Induced Tumor Apoptosis Using PEGylated, ^{111}In -Labeled Annexin V

Shi Ke, MD¹; Xiaoxia Wen, MS¹; Qing-Ping Wu, MD¹; Sidney Wallace, MD¹; Chusilp Charnsangavej, MD¹; Anne M. Stachowiak¹; Clifton L. Stephens, PhD²; James L. Abbruzzese, MD³; Donald A. Podoloff, MD¹; and Chun Li, PhD¹

¹Division of Diagnostic Imaging, University of Texas M.D. Anderson Cancer Center, Houston, Texas; ²Department of Surgical Oncology, University of Texas M.D. Anderson Cancer Center, Houston, Texas; and ³Department of Gastrointestinal Medical Oncology, University of Texas M.D. Anderson Cancer Center, Houston, Texas

$^{99\text{m}}\text{Tc}$ -Labeled annexin V has been used for the imaging of tumor apoptosis induced by chemotherapy. However, owing to the short half-life of annexin V, multiple injections of the radiotracer are necessary to capture the peak apoptotic activity. In this study, we evaluated the imaging properties of an ^{111}In -labeled, long-circulating annexin V. **Methods:** Both polyethylene glycol (PEG) and the metal chelator diethylenetriaminepentaacetic acid (DTPA) were simultaneously introduced to annexin V or ovalbumin through the use of a heterofunctional PEG precursor. Imaging studies were performed in mice bearing subcutaneously inoculated human mammary MDA-MB-468 tumors. The mice were treated with poly(L-glutamic acid)-paclitaxel, monoclonal antibody C225, or a combination of poly(L-glutamic acid)-paclitaxel and C225, followed by intravenous injection of ^{111}In -DTPA-PEG-annexin V. Images were acquired 48 h after the injection of the radiotracer. Autoradiography and TUNEL (terminal deoxynucleotidyltransferase-mediated dUTP nick-end labeling) staining were performed on adjacent tumor slices for the localization of apoptotic cells. The imaging properties of unPEGylated annexin V and PEGylated ovalbumin were also determined to permit assessment of the specificity of ^{111}In -DTPA-PEG-annexin V. **Results:** Tumor apoptotic index increased from $1.67\% \pm 0.31\%$ at baseline to $7.60\% \pm 0.72\%$ and $11.07\% \pm 1.81\%$, respectively, 4 d after treatment with poly(L-glutamic acid)-paclitaxel or combined poly(L-glutamic acid)-paclitaxel and C225. Tumor uptake (percentage of injected dose per gram of tumor [%ID/g]) of PEGylated ^{111}In -DTPA-PEG-annexin 4 d after treatment was significantly higher in tumors treated with poly(L-glutamic acid)-paclitaxel (10.76 ± 1.38 %ID/g; $P = 0.001$) and with combined poly(L-glutamic acid)-paclitaxel and C225 (9.84 ± 2.51 %ID/g; $P = 0.029$) than in nontreated tumors (6.14 ± 0.67 %ID/g), resulting in enhanced visualization of treated tumors. ^{111}In -DTPA-PEG-annexin V distributed into the central zone of tumors, whereas ^{111}In -DTPA-annexin V was largely confined to the tumor periphery. Furthermore, uptake of ^{111}In -DTPA-PEG-annexin V by tumors correlated with apoptotic index ($r = 0.87$, $P = 0.02$). Increase in tumor uptake of the nonspecific PEGylated protein ^{111}In -DTPA-PEG-ovalbumin was also observed after poly(L-glutamic acid)-paclitaxel treatment (55.6%), although this increase was less

than that observed for ^{111}In -DTPA-PEG-annexin V (96.7%). **Conclusion:** Increased uptake of and improved visualization with ^{111}In -DTPA-PEG-annexin V in solid tumors after chemotherapy are mediated through both specific binding to apoptotic cells and nonspecific retention of macromolecular contrast agents in the tumors. ^{111}In -Labeled, PEGylated annexin V may be used to assess tumor response to chemotherapy.

Key Words: apoptosis; nuclear imaging; annexin V; paclitaxel; polyethylene glycol

J Nucl Med 2004; 45:108–115

Recent data suggest that early cell death might be an important predictor of the success of chemotherapy. For example, Miltross et al. (1) found that the levels of paclitaxel-induced apoptosis correlated statistically with tumor growth delay. However, the role of apoptosis has generally been identified through histologic techniques, which are often limited by their invasive nature, by the heterogeneity of tumor sampling, and by the inaccessibility of some tumors. The ability to evaluate apoptosis by a noninvasive method might facilitate the clinical care of patients with cancer by abbreviating the time required to assess the potential efficacy of systemic treatment.

Owing to its high affinity to phosphatidylserine molecules that are exposed on the surface of apoptotic cells and other dead cells or cell fragments, annexin V has been proposed as a marker for noninvasive imaging of apoptosis (2). Blankenberg et al. (3) labeled annexin V directly with $^{99\text{m}}\text{Tc}$ through a small-molecular-weight chelator, hydrazinonicotinamide, and tested the ability of $^{99\text{m}}\text{Tc}$ -labeled annexin V to reveal apoptosis in a murine B-cell lymphoma tumor model. Unfortunately, no data about the intratumoral distribution of $^{99\text{m}}\text{Tc}$ -labeled annexin V were available with which to ascertain the correlation between apoptosis and tumor uptake of $^{99\text{m}}\text{Tc}$ -annexin V. Furthermore, owing to the short blood half-life of $^{99\text{m}}\text{Tc}$ -annexin V (<7 min) (2) and the short half-life of $^{99\text{m}}\text{Tc}$ radionuclide (6 h), it is difficult to extend the time of imaging using $^{99\text{m}}\text{Tc}$ -labeled annexin V beyond 6 h.

Received May 2, 2003; revision accepted Oct. 3, 2003.
For correspondence or reprints contact: Chun Li, PhD, Division of Diagnostic Imaging, Box 59, University of Texas M.D. Anderson Cancer Center, 1515 Holcombe Blvd., Houston, TX 77030.
E-mail: cli@di.mdacc.tmc.edu

Recent clinical studies by Belhocine et al. (4) demonstrated for the first time that overall survival and progression-free survival were significantly related to uptake of ^{99m}Tc -labeled annexin V in treated lung cancers and lymphomas. As noted by Blankenberg (5) in an accompanying editorial, the timing of annexin V imaging after a given therapy was critical. If peak apoptotic activity after anticancer therapy varies from patient to patient and from treatment to treatment, then it will be necessary to determine for each patient the best time to scan after the start of chemotherapy. It has been suggested that an imaging protocol using multiple separate injections of ^{99m}Tc -labeled annexin V and multiple radionuclide scans could be used to assess peak apoptotic activity (5). Such a protocol, however, may be difficult to implement in larger-scale trials.

We hypothesized that long-circulating annexin V may make it possible to capture therapy-induced apoptotic cells over a prolonged period. Thus, we have developed a simple procedure to synthesize polyethylene glycol (PEG)-modified, ^{111}In -labeled annexin V (6). PEG-modified proteins have been shown to exhibit reduced liver uptake and increased blood circulation half-lives, resulting in improved biologic activity (7,8). ^{111}In has a longer physical half-life (2.81 d) than ^{99m}Tc . In our previous study, we showed that PEGylated annexin V, ^{111}In -DTPA-PEG-annexin V (where DTPA is diethylenetriaminepentaacetic acid), selectively bound to apoptotic cells in vitro and had increased blood half-life in vivo. The half-life ($t_{1/2, \alpha}$) for PEGylated annexin V in nude mice was 4.90 h, whereas that of unPEGylated annexin V was only 0.07 h (6).

In this study, we sought to compare the imaging properties of ^{111}In -labeled PEGylated annexin V and ^{111}In -labeled unPEGylated annexin V in a mammary cancer xenograft.

MATERIALS AND METHODS

Materials

Annexin V (molecular weight, 33 kDa) was purchased from Sigma Chemical Co. Ovalbumin (molecular weight, 43 kDa) and PD-10 disposable columns were obtained from Amersham Biosciences. $^{111}\text{InCl}_3$ was obtained from Dupont-NEN. *p*-Isothiocyanatobenzyl-DTPA was obtained from Macrocyclics. *t*-Boc-PEG-NH₂ was obtained from Shearwater Polymers, Inc. Poly(L-glutamic acid)-paclitaxel (Xyotax) was a gift from Cell Therapeutics, Inc. Anti-epidermal growth factor receptor (EGFR) monoclonal antibody C225 was generously provided by Dr. Daniel J. Hicklin of ImClone Systems, Inc.

Synthesis and Radiolabeling of PEGylated Proteins

The PEG precursor containing an NH₂-reactive *p*-SCN group on one end and DTPA on the other end of the PEG chain, SCN-PEG-DTPA, was synthesized in accordance with procedures reported previously (6). To conjugate DTPA-PEG to proteins, aliquots of SCN-PEG-DTPA (15 μL , 0.18 μmol) in dimethylformamide were added to a solution of annexin V (0.40 mL, 0.006 μmol) or ovalbumin (0.52 mL, 0.006 μmol) in 0.1 mol/L phosphate-buffered saline (PBS) solution (pH 8.5), and the mixture was allowed to react at 4°C overnight. Unreacted SCN-PEG-DTPA was re-

moved using an AKTA fast-protein liquid chromatography system (Amersham Pharmacia Biotech) equipped with a Resource Q 1-mL anion-exchange column. The samples were eluted with 20 mmol/L Tris buffer (pH 7.5) and with a linear gradient of 0%–100% 1N NaCl in 15 mL at a flow rate of 4 mL/min. Sodium dodecyl sulfate-polyacrylamide gel electrophoresis (SDS-PAGE, 12%) was used to analyze the extent of protein PEGylation.

To label DTPA-PEG-annexin V and DTPA-PEG-ovalbumin with ^{111}In , a solution of DTPA-PEG-annexin V or DTPA-PEG-ovalbumin (300 μL , 200 $\mu\text{g}/\text{mL}$) in 20 mmol/L Tris buffer (pH 7.5) was incubated with 29.6 MBq (800 μCi) $^{111}\text{InCl}_3$ for 15 min. Free $^{111}\text{In}^{3+}$ was removed by gel filtration from a PD-10 column eluted with PBS. The purity of radiolabeled compound was analyzed by radio-gel permeation chromatography (GPC) and by gel electrophoresis. The GPC system consisted of an LDC pump (Laboratory Data Control), a LUDLUM radiometric detector (Measurement Inc.), and an SP 8450 UV/VIS detector (Spectra-Physics). The samples were separated using a Phenomenex Biosepe SEC-S3000 7.8 mm \times 30 cm column, eluted with PBS containing 0.1% LiBr at a flow rate of 1 mL/min, and detected by radioactivity and ultraviolet (UV) absorbance at 254 nm.

The SDS-PAGE gel was stained with Coomassie Brilliant Blue for the presence of proteins. For the detection of radioactivity, the dried gel was exposed to a multipurpose storage phosphor screen and analyzed using a Cyclone imager (Packard Instrument Co.).

Synthesis and Radiolabeling of DTPA-Annexin V

DTPA-annexin V was synthesized by reacting annexin V with *p*-SCN-DTPA in aqueous solution. PD-10 was used to remove unreacted DTPA. DTPA-annexin V was labeled with ^{111}In using the same procedures as described above. The purity of the radiotracer was examined by radio-GPC.

γ -Imaging with ^{111}In -DTPA-PEG-Annexin V

MDA-MB-468 tumor cells were grown as a monolayer in Dulbecco's modified Eagle's medium/F-12 medium supplemented with 10% fetal bovine serum. Female nude mice, 18–22 g (Harlan Sprague-Dawley), were inoculated subcutaneously in the anterior chest wall with 1.5×10^6 MDA-MB-468 cells per site. When the tumors had grown to 200 mm³ in average volume, the mice were assigned to groups of 3 mice each. Groups of mice were given a single intravenous injection of poly(L-glutamic acid)-paclitaxel at a dose of 25 mg equivalent (eq) paclitaxel/kg, a single intravenous injection of poly(L-glutamic acid)-paclitaxel at a dose of 100 mg eq paclitaxel/kg, intraperitoneal injections of C225 at a dose of 1 mg per mouse per injection on day 1 and day 4, combined treatment with poly(L-glutamic acid)-paclitaxel (100 mg eq paclitaxel/kg) and C225 (1 mg per mouse per injection), or no treatment control. On day 1 or day 4 after the initiation of treatment, mice were injected with ^{111}In -DTPA-PEG-annexin V (8 μg eq annexin V per mouse; 1.85 MBq [50 μCi] per mouse) through the tail vein.

Forty-eight hours after injection of the radiotracer (day 3 and day 6 after initiation of treatment), planar γ -images were acquired in a 64 \times 64 matrix for 5 min using a solid-state γ -camera (model 2020tc; DigiRad) equipped with a medium-energy collimator and Mirage processing software (version 4.322; Segami Corp.). The mice were placed prone on the camera's parallel-hole collimator after they were anesthetized with an intraperitoneal injection of sodium pentobarbital (35 mg/kg). At the end of the imaging session, the mice were killed and tumors were removed from each animal for radioactivity measurements and autoradiography. Tu-

mor uptake of ^{111}In -DTPA-PEG-annexin V was expressed as percentage of the injected dose per gram of tissue (%ID/g tissue).

Determination of Apoptotic Index

Mice bearing MD-MB-468 tumors were killed at different times after treatments, and the tumors were immediately excised and placed in neutral-buffered formalin. The tissues were then processed and stained with hematoxylin–eosin (H&E) stain. Apoptosis was scored in coded slides by microscopic examination at $\times 400$ magnification according to the method of Milas et al. (9). Briefly, 5 fields of nonnecrotic areas were randomly selected in each histologic specimen, and, in each field, the number of apoptotic nuclei per 100 nuclei examined was determined and expressed as a percentage. The values were based on scoring 1,500 nuclei obtained from 3 mice per time point.

Autoradiography

Tumors removed from mice injected with ^{111}In -DTPA-PEG-annexin V or ^{111}In -DTPA-annexin V at the end of the γ -imaging session (4 d after radiotracer injection) were immediately frozen and processed. Sliced 8- μm sections were fixed in cold acetone, dried, and exposed to a multipurpose storage phosphor screen for 10 d. A Cyclone storage phosphor screen imager (Packard Instrument Co.) was used to detect the distribution of radionuclide activity localized in each section.

TUNEL Assay

DNA fragmentation was analyzed by terminal deoxynucleotidyltransferase-mediated dUTP nick-end labeling (TUNEL) assay using a commercial kit (Promega) according to the manufacturer's protocol. Briefly, frozen tissue sections (8 μm) were fixed with 4% methanol-free paraformaldehyde for 10 min at room temperature. The sections were washed and incubated sequentially with equilibration buffer and reaction buffer containing nucleotide mixture and terminal deoxynucleotidyltransferase. To prevent photobleaching, Vectashield mounting medium (Vector Laboratories, Inc.) was used to mount coverslips. Images were recorded using an Olympus fluorescence microscope with a 520-nm filter and an $\times 20$ objective lens.

Biodistribution Studies

Mice bearing MDA-MB-468 tumors were assigned to groups of 3 mice each. Mice in each of the 3 treated groups were given a single intravenous injection of poly(L-glutamic acid)-paclitaxel at a dose of 100 mg eq paclitaxel/kg. Mice in each of the 3 control groups were not treated. Four days after drug treatment, mice in control groups and treated groups were injected with ^{111}In -DTPA-PEG-annexin V (4 μg eq annexin V per mouse; 1.48 MBq [40 μCi] per mouse), ^{111}In -DTPA-PEG-ovalbumin (4 μg eq ovalbumin per mouse; 1.48 MBq [40 μCi] per mouse), or ^{111}In -DTPA-annexin V (4 μg eq annexin V per mouse; 1.11 MBq [30 μCi] per mouse). No cold carriers were added to the radiotracers. γ -Images were acquired in a 64×64 matrix for 15 min at 4 and 48 h after the injection of each radiotracer using a Siemens m.Cam γ -camera equipped with a medium-energy, low-penetration collimator and ICON software version 9.5. Mice were prepared for the imaging sessions as described before. At the end of the imaging session, the mice were killed, and various tissues were removed from each animal for radioactivity measurements. The data were expressed as %ID/g tissue.

Data Analysis

Statistical comparisons between untreated controls and each treated group for each radiotracer were calculated using the Student *t* test. $P < 0.05$ was considered to be statistically significant. The Pearson correlation coefficient was used to assess the correlation between the average tumor uptake of ^{111}In -DTPA-PEG-annexin V and the average apoptotic index. Five treatment groups, each consisting of 3 mice, were used to derive the correlation curve.

RESULTS

Synthesis and Radiolabeling of PEGylated Proteins

Analysis of reaction products resulting from mixture of annexin V or ovalbumin with SCN-PEG-DTPA using 12% SDS-PAGE revealed quantitative conversion of annexin V and ovalbumin to PEGylated proteins (Fig. 1). The molecular weight of DTPA-PEG-annexin V was estimated to be between 81 and 114 kDa on the basis of SDS-PAGE data, suggesting that PEGylated annexin V in each preparation contained 10–16 PEG molecules.

On radio-GPC, the radioactivity peaks and the corresponding UV absorbance peaks for ^{111}In -DTPA-PEG-annexin V and ^{111}In -DTPA-PEG-ovalbumin appeared at the same retention volumes, indicating successful radiolabeling of PEGylated proteins. No free ^{111}In -DTPA-PEG was detected in either product (data not shown). SDS-PAGE analysis of ^{111}In -DTPA-PEG-annexin V further confirmed the successful radiolabeling of PEGylated annexin V. Figure 1

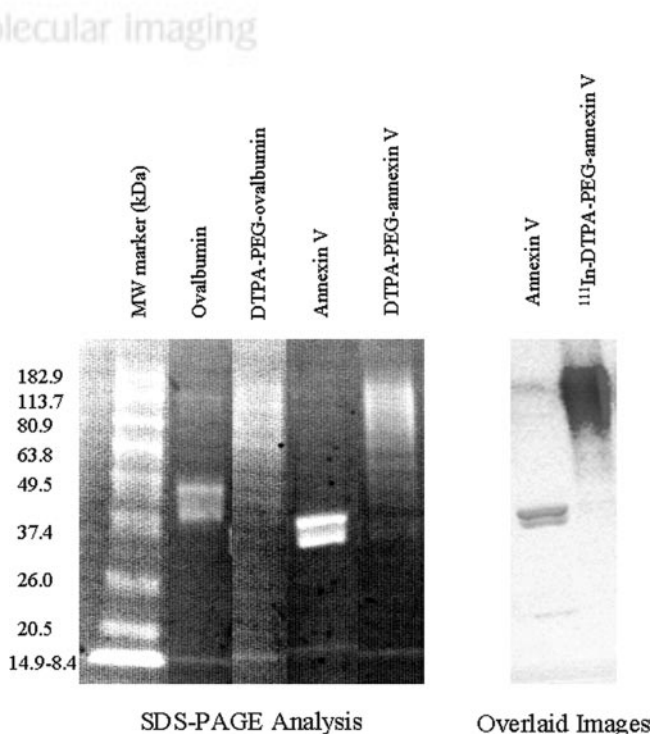


FIGURE 1. SDS-PAGE analysis of DTPA-PEG-annexin V and DTPA-PEG-ovalbumin. Overlaid images of ^{111}In -DTPA-PEG-annexin V protein and radioactivity are also shown. No free annexin V or small-molecular-weight contaminants were present in DTPA-PEG-annexin V or ^{111}In -DTPA-PEG-annexin V preparations. MW = molecular weight.

shows the overlaid images of protein stained with Coomassie Brilliant Blue and radioactivity detected by the Cyclone imager. The radioactivity was associated only with the ^{111}In -DTPA-PEG-annexin V band (Fig. 1). The radiochemical yield for both ^{111}In -DTPA-PEG-annexin V and ^{111}In -DTPA-PEG-ovalbumin was 85%–91%. Specific activity was 296–370 kBq (8–10 $\mu\text{Ci}/\mu\text{g}$).

DTPA-annexin V was synthesized from annexin V and *p*-SCN-DTPA. The radiochemical yield and radiochemical purity of ^{111}In -DTPA-annexin V were 74% and >98%, respectively. The specific activity was 296 kBq (8 $\mu\text{Ci}/\mu\text{g}$).

γ -Imaging with ^{111}In -DTPA-PEG-Annexin V

To validate the use of ^{111}In -DTPA-PEG-annexin V for the noninvasive imaging of tumor apoptosis, we first evaluated whether ^{111}In -DTPA-PEG-annexin V could capture apoptotic responses of MDA-MB-468 tumors to poly(L-glutamic acid)-paclitaxel and C225 treatments. γ -Images acquired 48 h after radiotracer injection clearly showed increased radioactivity in the gastrointestinal tract as well as in the tumors of mice treated with either poly(L-glutamic acid)-paclitaxel at a dose of 100 mg eq paclitaxel/kg or combined poly(L-glutamic acid)-paclitaxel and C225 therapy given 4 d before radiotracer injection compared with the radioactivity in tumors of untreated mice (Figs. 2A–2C). Treatment with poly(L-glutamic acid)-paclitaxel at a dose of 25 mg eq paclitaxel/kg did not result in apparent enhancement in tumor uptake of ^{111}In -DTPA-PEG-annexin V (data not shown). Similarly, treatment with C225 alone did not cause detectable change in tumor uptake of the radiotracer (Fig. 2D). These observations were confirmed by scintillation well counting. Treatments with poly(L-glutamic acid)-paclitaxel at a dose of 100 mg eq paclitaxel/kg poly(L-glutamic acid)-paclitaxel or combined poly(L-glutamic acid)-paclitaxel and C225 increased the tumor uptake of ^{111}In -DTPA-PEG-annexin V by 75% ($P = 0.001$) and 60% ($P = 0.029$), respectively, when the radiotracer was injected

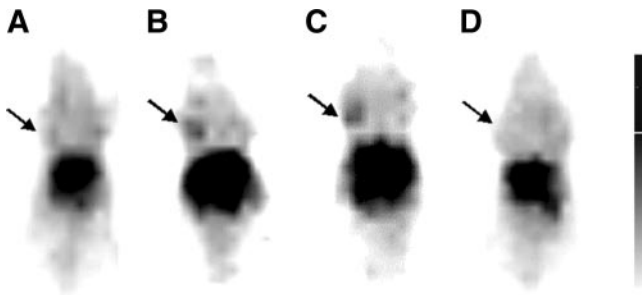


FIGURE 2. Representative γ -images of mice with MDA-MB-468 tumors 48 h after intravenous injection of ^{111}In -DTPA-PEG-annexin V. Mice were not treated (A) or were treated with poly(L-glutamic acid)-paclitaxel at 100 mg eq paclitaxel/kg (B), combined poly(L-glutamic acid)-paclitaxel and C225 therapy (C), or C225 at 1 mg per mouse per injection on day 1 and day 4 (D). All treatments were initiated 4 d before injection of radiotracer. Images were acquired from different animals. Arrows: tumor.

TABLE 1
Apoptotic Index and Tumor Uptake of ^{111}In -DTPA-PEG-Annexin V in MDA-MB-468 Tumors After Drug Treatments

Treatment*	Apoptosis index [†]	Tumor uptake (%ID/g) [‡]
Control	1.67 \pm 0.31	6.14 \pm 0.67
Poly(L-glutamic acid)-paclitaxel (1 d)	4.33 \pm 0.31 [§]	6.95 \pm 1.11
Poly(L-glutamic acid)-paclitaxel (4 d)	7.60 \pm 0.72 [§]	10.76 \pm 1.38 [§]
C225 (1 d)	2.73 \pm 0.46 [¶]	6.99 \pm 1.49
C225 (4 d)	1.93 \pm 0.50	4.69 \pm 0.54 [¶]
Poly(L-glutamic acid)-paclitaxel/C225 (4 d)	11.07 \pm 1.81 [§]	9.84 \pm 2.51 [¶]

*Poly(L-glutamic acid)-paclitaxel was given intravenously at dose of 100 mg eq paclitaxel/kg; C225 was given intraperitoneally at dose of 1 mg per mouse per injection.

[†]Apoptosis index for cancer cells is expressed as mean percentage \pm SD of values from 3 mice. For each mouse, apoptosis index was determined from average of percentage of apoptotic nuclei within 5 randomly selected $\times 400$ fields.

[‡]%ID/g of tumor. Data are presented as mean percentage \pm SD of values from 3 mice.

[§] $P < 0.001$ vs. control (Student *t* test).

[¶] $P < 0.05$ vs. control (Student *t* test).

Data were obtained 48 h after radiotracer injection.

4 d after the initiation of drug treatment. On the other hand, treatment with C225 alone significantly decreased the tumor uptake of ^{111}In -DTPA-PEG-annexin V by 24% ($P = 0.028$) (Table 1). No differences were found in tumor uptake of ^{111}In -DTPA-PEG-annexin V between control mice and mice treated with poly(L-glutamic acid)-paclitaxel or C225 when the radiotracer was injected 1 d after the initiation of drug treatment (Table 1).

Correlation Between Tumor Uptake and Drug-Induced Apoptosis

To investigate whether tumor uptake of ^{111}In -DTPA-PEG-annexin V correlated with drug-induced apoptosis, we compared tumor uptake of ^{111}In -DTPA-PEG-annexin V with the drug-induced apoptotic index. We also compared the intratumoral distribution of radioactivity due to ^{111}In -DTPA-PEG-annexin V (determined by autoradiography) and apoptosis (determined by TUNEL staining).

Histologic analysis of H&E-stained tumor tissues revealed that poly(L-glutamic acid)-paclitaxel and combined poly(L-glutamic acid)-paclitaxel and C225 significantly increased the percentage of apoptotic cells at 4 d after drug injection. The apoptotic index at that time was 1.67% \pm 0.31% in untreated tumors, 7.6% \pm 0.72% in poly(L-glutamic acid)-paclitaxel-treated tumors ($P < 0.001$), and 11.07% \pm 1.81% in tumors treated with both poly(L-glutamic acid)-paclitaxel and C225 ($P < 0.001$) (Table 1). Treatment with C225 alone had no effect on the apoptotic index ($P = 0.48$). Importantly, there was a significant correlation between tumor uptake of ^{111}In -DTPA-PEG-annexin

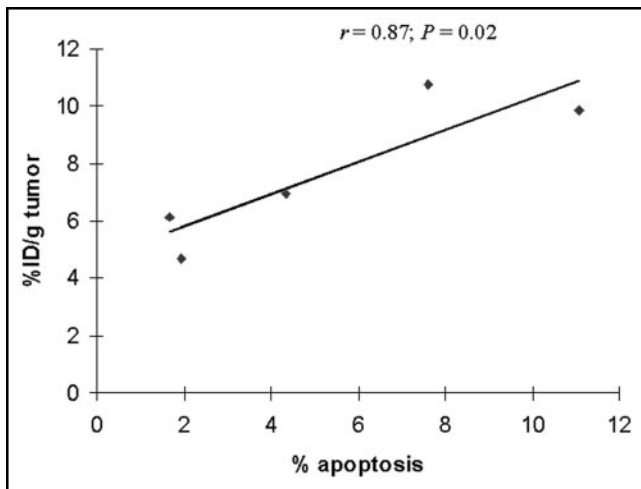


FIGURE 3. Correlation between %ID/g of ^{111}In -DTPA-PEG-annexin V and apoptotic index determined histologically.

V expressed as %ID/g and apoptotic index determined histologically ($r = 0.87$; $P = 0.02$) (Fig. 3).

Intratumoral Distribution of ^{111}In -DTPA-PEG-Annexin V

Autoradiograms of tumors excised from mice treated with poly(L-glutamic acid)-paclitaxel, C225, or poly(L-glutamic acid)-paclitaxel and C225 and injected with ^{111}In -DTPA-PEG-annexin V or ^{111}In -DTPA-annexin V 4 d after drug injection are presented in Figure 4. Among mice injected with ^{111}In -DTPA-PEG-annexin V, in tumors from untreated mice, radioactivity was localized primarily in the periphery of the tumors, with little activity found in the central zone (Fig. 4). However, in tumors from mice treated with poly(L-glutamic acid)-paclitaxel and poly(L-glutamic acid)-paclitaxel and C225, significant radioactivity was found in the central zone as well as in the periphery (Fig. 4). Tumor uptake of ^{111}In -DTPA-PEG-annexin V in mice treated with C225 alone was reduced compared with that in untreated mice (Fig. 4). In tumors of mice injected with ^{111}In -DTPA-annexin V, the radioactivity was much weaker than in tumors of mice injected with ^{111}In -DTPA-PEG-annexin V, and the activity was mainly confined to the tumor periphery (Fig. 4).

The TUNEL-positive apoptotic cells and radioactivity from ^{111}In -DTPA-PEG-annexin V were heterogeneously distributed in tumors. Intense TUNEL staining colocalized

FIGURE 4. Intratumoral distribution of ^{111}In -DTPA-PEG-annexin V and ^{111}In -DTPA-annexin V in tumors from untreated mice (Control) and from mice treated with poly(L-glutamic acid)-paclitaxel (Xyotax) at a dose of 100 mg eq paclitaxel/kg, combined poly(L-glutamic acid)-paclitaxel and C225 (Xyotax/C225), or C225 alone at dose of 1 mg per mouse per injection. All treatments were initiated 4 d before injection of each radiotracer. Animals were killed 48 h after injection of each radiotracer.

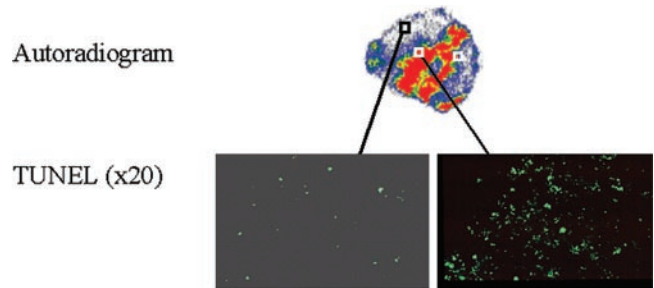
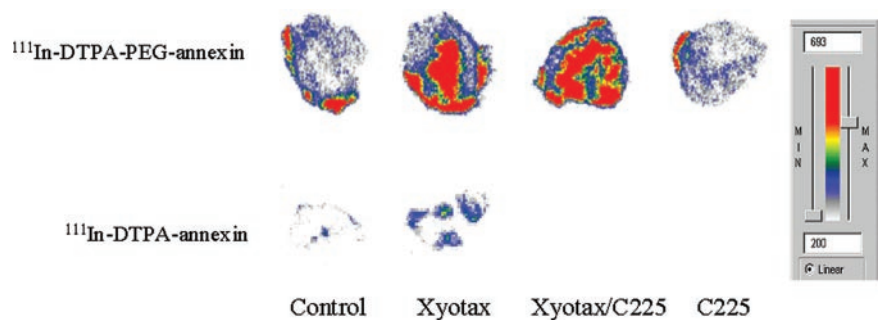


FIGURE 5. Representative autoradiogram and TUNEL staining results for adjacent tumor sections from mice treated with combined poly(L-glutamic acid)-paclitaxel and C225. ^{111}In -DTPA-PEG-annexin V was injected intravenously 4 d after initiation of drug treatment. Note colocalization of hot spot with intense positive TUNEL staining (right) and cold spot with scarce TUNEL staining (left).

with hot spots from ^{111}In -DTPA-PEG-annexin V, whereas weak TUNEL staining corresponded to cold spots with low radioactivity (Fig. 5).

Imaging with ^{111}In -DTPA-Annexin V and ^{111}In -DTPA-PEG-Ovalbumin

γ -Imaging with ^{111}In -DTPA-annexin V failed to reveal tumors in either untreated mice or mice treated with poly(L-glutamic acid)-paclitaxel (Fig. 6, left). At 4 h after radiotracer injection, ^{111}In -DTPA-annexin V was primarily taken up by the kidney (Table 2), and there was little blood-pool activity. As in the case of ^{111}In -DTPA-PEG-annexin V (Fig. 2B is representative image), mice injected with ^{111}In -DTPA-PEG-ovalbumin had visible background blood-pool activity at 48 h after radiotracer injection (Fig. 6, right). Tumors were visualized with ^{111}In -DTPA-PEG-ovalbumin in both untreated and treated mice. However, changes in tumor uptake in untreated and poly(L-glutamic acid)-paclitaxel-treated mice could not be discerned with ^{111}In -DTPA-PEG-ovalbumin, whereas increased activity in tumors of poly(L-glutamic acid)-paclitaxel-treated mice was clearly visualized with ^{111}In -DTPA-PEG-annexin V (Fig. 2).

Biodistribution

Tissue distributions of ^{111}In -DTPA-PEG-annexin V, ^{111}In -DTPA-PEG-ovalbumin, and ^{111}In -DTPA-annexin V in untreated mice and poly(L-glutamic acid)-paclitaxel-treated mice at 48 h after radiotracer injection are summarized in

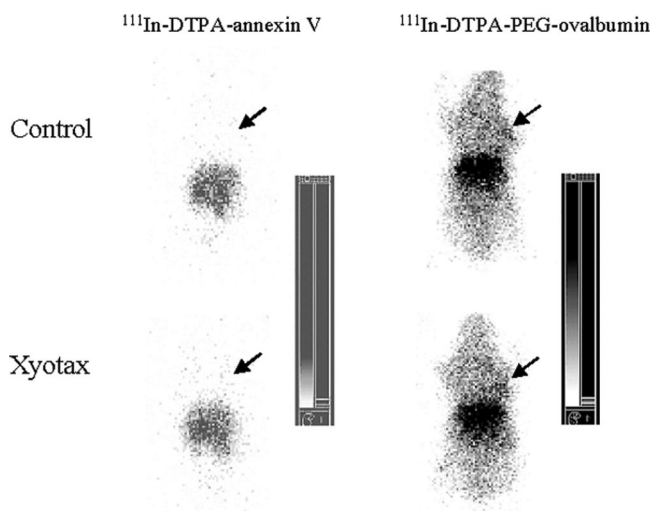


FIGURE 6. γ -Images of mice injected with ^{111}In -DTPA-annexin V and ^{111}In -DTPA-PEG-ovalbumin. Mice were either not treated (Control) or treated with poly(L-glutamic acid)-paclitaxel (Xyotax) at dose of 100 mg eq paclitaxel/kg given 4 d before injection of each radiotracer. Images were acquired 4 h after injection of ^{111}In -DTPA-annexin V or 48 h after injection of ^{111}In -DTPA-PEG-ovalbumin. Arrows: tumor.

Table 2. Treatment with poly(L-glutamic acid)-paclitaxel resulted in a significant increase in tumor uptake of ^{111}In -DTPA-PEG-annexin V ($P = 0.033$) and ^{111}In -DTPA-PEG-ovalbumin ($P = 0.028$) (Table 2). Comparing treated and untreated mice, the tumor uptake of ^{111}In -DTPA-PEG-annexin V increased 96.7% (from 8.13% to 15.99%), and the tumor uptake of ^{111}In -DTPA-PEG-ovalbumin increased 55.6% (from 9.08% to 14.13%). The tumor-to-blood and tumor-to-muscle ratios in mice injected with ^{111}In -DTPA-PEG-annexin V increased 92% and 96%, respectively. In contrast, the tumor-to-blood and tumor-to-muscle ratios in

mice injected with ^{111}In -DTPA-PEG-ovalbumin only changed -2% and 17% , respectively (Table 2).

The distribution pattern of unPEGylated ^{111}In -DTPA-annexin V was different from that of the PEGylated proteins (Table 2). ^{111}In -DTPA-annexin V did show increased tumor uptake after poly(L-glutamic acid)-paclitaxel treatment. However, the uptake value for ^{111}In -DTPA-annexin V (1.23 %ID/g) was much lower than that of ^{111}In -DTPA-PEG-annexin V (15.99 %ID/g) after poly(L-glutamic acid)-paclitaxel treatment. Similarly, the tumor-to-muscle ratio for ^{111}In -DTPA-annexin V (3.62-fold) was much lower than that for ^{111}In -DTPA-PEG-annexin V (13.2-fold) (Table 2).

DISCUSSION

Owing to its short blood half-life (<7 min) and a relatively high molecular weight (>30 kDa), $^{99\text{m}}\text{Tc}$ -labeled annexin V is likely confined to areas with relatively good blood perfusion. Limited exposure time and penetration into solid tumors may compromise the sensitivity of nuclear imaging with $^{99\text{m}}\text{Tc}$ -labeled annexin V. In fact, in the study by Blankenberg et al. (3), murine B-cell lymphoma in mice treated with cyclophosphamide showed a 2.3-fold increase in annexin V uptake compared with untreated control, whereas histologic analysis showed a >19 -fold increase in apoptosis after treatment, suggesting that the technique is not a very sensitive one. We hypothesized that increasing the blood half-life of annexin V may allow radiolabeled annexin V to penetrate deep into the tumor mass. Furthermore, apoptosis is a dynamic process in which newly generated apoptotic cells are rapidly removed by phagocytic macrophages (10). Snapshots of apoptotic cells identified through histologic techniques or a rapid imaging session performed shortly after radiotracer injection may not permit a clear delineation over the time line of apoptosis in the course of treatment. Increasing the interval between radio-

TABLE 2
Distribution of ^{111}In -DTPA-PEG-annexin V, ^{111}In -DTPA-PEG-ovalbumin, and ^{111}In -DTPA-annexin V

Radiotracer and Treatment*	Blood	Liver	Kidney	Muscle	Tumor	Ratio	
						Tumor-to-blood	Tumor-to-muscle
^{111}In-DTPA-PEG-annexin V							
No treatment	4.44 \pm 0.53	46.92 \pm 4.48	35.73 \pm 3.87	1.21 \pm 0.06	8.13 \pm 0.28	1.83	6.72
Poly(L-glutamic acid)-paclitaxel	4.56 \pm 0.64	49.24 \pm 7.70	27.22 \pm 4.36	1.21 \pm 0.25	15.99 \pm 4.27 [†]	3.51	13.2
^{111}In-DTPA-PEG-ovalbumin							
No treatment	2.28 \pm 0.14	22.45 \pm 1.71	24.00 \pm 1.27	1.15 \pm 0.15	9.08 \pm 1.72	3.98	7.89
Poly(L-glutamic acid)-paclitaxel	3.63 \pm 0.31	27.76 \pm 2.67	22.82 \pm 1.56	1.53 \pm 0.15	14.13 \pm 0.44 [†]	3.89	9.23
^{111}In-DTPA-annexin V							
No treatment	0.03 \pm 0.01	10.33 \pm 1.07	150.0 \pm 12.1	0.19 \pm 0.06	0.62 \pm 0.14	20.67	3.26
Poly(L-glutamic acid)-paclitaxel	0.03 \pm 0.02	6.03 \pm 4.15	145.7 \pm 55.2	0.34 \pm 0.20	1.23 \pm 0.67	41.00	3.62

Data were obtained 48 h after radiotracer injection and are expressed as %ID/g of tissue. Each data point represents mean \pm SD from 3 mice.

*Poly(L-glutamic acid)-paclitaxel was given intravenously at dose of 100 mg eq paclitaxel/kg 4 d before injection of each radiotracer.

[†] $P < 0.05$ compared with corresponding untreated group.

tracer injection and image acquisition would allow capturing of apoptotic cells produced over a period of time, leading to improved detection sensitivity.

In this study, we evaluated the *in vivo* imaging properties of ^{111}In -labeled, PEGylated annexin V in mice bearing human mammary MDA-MB-468 tumors. Tumor apoptosis was induced by treatments with a water-soluble taxane, poly(L-glutamic acid)-paclitaxel, and with monoclonal antibody C225. Poly(L-glutamic acid)-paclitaxel is a polymeric paclitaxel conjugate that has demonstrated significant antitumor activity with reduced systemic toxicity in preclinical and clinical studies (11). The conjugate is currently being evaluated in several clinical phase I–III trials. C225 is a human–mouse chimeric monoclonal antibody that targets the EGFRs (12). C225 inhibits EGFR tyrosine kinase activity, proliferation, and tumor-induced angiogenesis in a variety of cultured and xenografted human cancer cells that express high levels of EGFR (12–14). Exposure of MDA-MB-468 cells to C225 inhibits cell proliferation but does not induce caspase-8 activation and apoptosis (15). Recent reports indicate that C225 modulates host responses and enhances the efficacy of paclitaxel (16).

We found that treatment with poly(L-glutamic acid)-paclitaxel or combined poly(L-glutamic acid)-paclitaxel and C225 significantly increased the uptake of ^{111}In -DTPA-PEG-annexin V in tumors (Fig. 2; Table 1). The specificity of the detection was confirmed by strong correlation between the tumor uptake of ^{111}In -DTPA-PEG-annexin V and the apoptosis index determined histologically (Fig. 3) and by colocalization of the radioactivity associated with ^{111}In -DTPA-PEG-annexin V and tumor apoptosis revealed by TUNEL staining (Fig. 5).

The advantage of PEGylated annexin V over unPEGylated annexin V was demonstrated by comparing images obtained with ^{111}In -DTPA-PEG-annexin V and ^{111}In -DTPA-annexin V. Whereas no tumors were detectable before or after poly(L-glutamic acid)-paclitaxel treatment at 4 h after ^{111}In -DTPA-annexin V injection (Fig. 6), enhanced tumor uptake of ^{111}In -DTPA-PEG-annexin V was clearly visualized in poly(L-glutamic acid)-paclitaxel-treated mice 48 h after radiotracer injection (Fig. 2). Imaging with DTPA-annexin V at 48 h after radiotracer injection also failed to delineate tumors in mice treated with poly(L-glutamic acid)-paclitaxel (data not shown). The fraction of apoptotic cells in MDA-MB-468 tumors after poly(L-glutamic acid)-paclitaxel treatment was quite low, 7.6%–11.1% (Table 1), indicating that ^{111}In -DTPA-PEG-annexin V is sensitive in the detection of apoptotic cells. It is plausible that increased exposure to ^{111}In -DTPA-PEG-annexin V may have contributed to the enhanced detection sensitivity compared with ^{111}In -DTPA-annexin V. Alternatively, the increased blood half-life of ^{111}In -DTPA-PEG-annexin V could have allowed the radiotracer to diffuse deeper into the tumor mass than ^{111}In -DTPA-annexin V could. This is supported by comparing autoradiographs of tumors from mice injected with ^{111}In -DTPA-PEG-annexin

V and ^{111}In -DTPA-annexin V (Fig. 4). Poly(L-glutamic acid)-paclitaxel treatment resulted in strong radioactivity in the central zone in addition to the peripheral zone of tumors from mice injected with ^{111}In -DTPA-PEG-annexin V; in contrast, only weak radioactivity was found in the periphery of tumors from mice treated with poly(L-glutamic acid)-paclitaxel and injected with ^{111}In -DTPA-annexin V (Fig. 4). For both radiolabeled annexin V radiotracers, a potential limitation is on its utility in abdominal imaging. The high accumulation of the radiotracer in the liver and kidney might preclude the use of these agents for abdominal imaging.

To evaluate whether the uptake of PEGylated annexin V was related to nonspecific uptake of macromolecules owing to the enhanced permeability and retention (EPR) effect (11), we compared tumor uptake of ^{111}In -DTPA-PEG-annexin V with tumor uptake of the nonspecific PEGylated protein, ^{111}In -DTPA-PEG-ovalbumin. Ovalbumin has a molecular weight of 43 kDa, which is close to that of annexin V (33 kDa). γ -Imaging of MDA-MB-468 tumor-bearing mice with ^{111}In -DTPA-PEG-ovalbumin showed the presence of tumors before and after poly(L-glutamic acid)-paclitaxel treatment, although it is difficult to ascertain whether poly(L-glutamic acid)-paclitaxel treatment led to enhanced tumor uptake of the radiotracer (Fig. 6). Scintillation well counting showed that both ^{111}In -DTPA-PEG-annexin V and ^{111}In -DTPA-PEG-ovalbumin had high blood-pool activity at 48 h after radiotracer injection (Table 2). Treatment with poly(L-glutamic acid)-paclitaxel resulted in a 96.7% increase in the tumor uptake of ^{111}In -DTPA-PEG-annexin V and a 55.6% increase in the tumor uptake of ^{111}In -DTPA-PEG-ovalbumin, suggesting that a fraction of the increased tumor uptake of ^{111}In -DTPA-PEG-annexin V after poly(L-glutamic acid)-paclitaxel treatment was due to the nonspecific EPR effect of macromolecules (Table 2). Importantly, only ^{111}In -DTPA-PEG-annexin V ($P < 0.005$) but not ^{111}In -DTPA-PEG-ovalbumin showed a significant increase in the tumor-to-blood ratio and the tumor-to-muscle ratio between the poly(L-glutamic acid)-paclitaxel-treated group and the nontreated control group (Table 2).

It is interesting to note that C225 treatment alone resulted in a 33% reduction in the tumor uptake of ^{111}In -DTPA-PEG-annexin V 4 d after the initiation of the treatment (Table 1). Similarly, combined poly(L-glutamic acid)-paclitaxel and C225 therapy result in less tumor uptake of ^{111}In -DTPA-PEG-annexin V than poly(L-glutamic acid)-paclitaxel treatment alone. These results are consistent with the finding that C225 is not a potent inducer of apoptosis (15,16). Inoue et al. (16) found that in bladder tumor xenografts, C225 but not paclitaxel significantly reduced microvessel density counts. It is possible that the reduced tumor uptake of ^{111}In -DTPA-PEG-annexin V in mice treated with C225 may reflect reduced blood vessel permeability, which is secondary to downregulation of EGFR, vascular endothelial growth factor receptor, and the expression of other angiogenic factors (16).

CONCLUSION

In this study, we evaluated the potential application of long-circulating, PEGylated annexin V for imaging drug-induced cell death. We observed increased uptake and improved visualization with ^{111}In -DTPA-PEG-annexin V in solid tumors after taxane treatments. These results are probably mediated through both specific binding to apoptotic cells and nonspecific retention of macromolecular contrast agents in the tumors. Thus, ^{111}In -labeled, PEGylated annexin V may be used to assess tumor response to chemotherapy.

ACKNOWLEDGMENTS

The authors thank Dr. Richard Wendt and Scott Miller for their help in acquisition and processing of γ -imaging data and Dr. Tarik Belhocine for helpful discussion. We also thank Stephanie Deming for help in editing the manuscript. This research was supported in part by National Institutes of Health (NIH) grant U54 CA090810 and by the John S. Dunn Foundation. Nuclear magnetic resonance studies and animal experiments were supported by NIH Cancer Center support grant CA16672.

REFERENCES

1. Miltross CG, Mason KA, Hunter NR, Chung W-K, Peters LJ, Milas L. Relationship of mitotic arrest and apoptosis to antitumor effect of paclitaxel. *J Natl Cancer Inst.* 1996;88:1308–1314.
2. Blankenberg FG, Tait J, Ohtsuki K, Strauss HW. Apoptosis, the importance of nuclear medicine. *Nucl Med Commun.* 2001;21:241–250.
3. Blankenberg FG, Katsikis P, Tait JF, et al. In vivo detection and imaging of phosphatidylserine expression during programmed cell death. *Proc Natl Acad Sci USA.* 1998;95:6349–6354.
4. Belhocine T, Steinmetz N, Hustinx R, et al. Increased uptake of the apoptosis-imaging agent $^{99\text{m}}\text{Tc}$ recombinant human annexin V in human tumors after one course of chemotherapy as a predictor of tumor response and patient prognosis. *Clin Cancer Res.* 2002;8:2766–2774.
5. Blankenberg F. To scan or not to scan, it is a question of timing: technetium-99m-annexin V radionuclide imaging assessment of treatment efficacy after one course of chemotherapy [editorial]. *Clin Cancer Res.* 2002;8:2757–2758.
6. Wen X-X, Wu Q-P, Ke S, et al. Improved radiolabeling of PEGylated protein: PEGylated annexin V for noninvasive imaging of tumor apoptosis. *Cancer Biother Radiopharm.* 2003;18:819–827.
7. Fuertges F, Abuchowski A. The clinical efficacy of poly(ethylene glycol)-modified proteins. *J Control Release.* 1990;11:139–148.
8. Chapman AP, Antoniow P, Spitali M, West S, Stephens S, King DJ. Therapeutic antibody fragments with prolonged in vivo half-lives. *Nat Biotechnol.* 1999;17:780–783.
9. Milas L, Hunter NR, Kurdoglu B, et al. Kinetics of mitotic arrest and apoptosis in murine mammary and ovarian tumors treated with taxol. *Cancer Chemother Pharmacol.* 1995;35:297–303.
10. Green DR, Beere HM. Gone but not forgotten. *Nature.* 2000;405:28–29.
11. Li C. Poly(L-glutamic acid)-anticancer drug conjugates. *Adv Drug Delivery Rev.* 2002;54:695–713.
12. Mendelsohn J. Epidermal growth factor receptor inhibition by a monoclonal antibody as anticancer therapy. *Clin Cancer Res.* 1997;3:2703–2707.
13. Fan Z, Masui H, Altas I, Mendelsohn J. Blockage of epidermal growth factor receptor function by bivalent and monovalent fragments of 225 anti-epidermal growth factor receptor monoclonal antibodies. *Cancer Res.* 1993;53:4322–4328.
14. Perrotte P, Matsumoto T, Inoue K, et al. Anti-epidermal growth factor receptor antibody C225 inhibits angiogenesis in human transitional cell carcinoma growing orthotopically in nude mice. *Clin Cancer Res.* 1999;5:257–265.
15. Liu B, Fan Z. The monoclonal antibody 225 activates caspase-8 and induces apoptosis through a tumor necrosis factor receptor family-dependent pathway. *Oncogene.* 2001;20:3726–3734.
16. Inoue K, Slaton JW, Perrotte P, et al. Paclitaxel enhances the effects of the anti-epidermal growth factor receptor monoclonal antibody ImClone C225 in mice with metastatic human bladder transitional cell carcinoma. *Clin Cancer Res.* 2000;6:6874–6884.